Journal of Experimental and Theoretical Physics, Vol. 96, No. 5, 2003, pp. 857–869.
Translated from Zhurnal Éksperimental'noĭ i Teoreticheskoĭ Fiziki, Vol. 123, No. 5, 2003, pp. 975–990.

ATOMS, SPECTRA, RADIATION

Waveguide Modes of Electromagnetic Radiation in Hollow-Core Microstructure and Photonic-Crystal Fibers

S. O. Konorov[a], O. A. Kolevatova[a], A. B. Fedotov[a,b], E. E. Serebryannikov[a], D. A. Sidorov-Biryukov[b], J. M. Mikhailova[a], A. N. Naumov[b], V. I. Beloglazov[c], N. B. Skibina[c], L. A. Mel'nikov[c], A. V. Shcherbakov[c], and A. M. Zheltikov [a,b]

[a] *Physics Department, M. V. Lomonosov Moscow State University, Vorob'evy gory, 119899 Moscow, Russia*
e-mail: zheltikov@top.phys.msu.su
[b] *International Laser Center, M. V. Lomonosov Moscow State University, Vorob'evy gory, 119899 Moscow, Russia*
[c] *Technology and Equipment for Glass Structures Institute, pr. Stroitelei 1, 410044 Saratov, Russia*
Received October 31, 2002

Abstract—The properties of waveguide modes in hollow-core microstructure fibers with two-dimensionally periodic and aperiodic claddings are studied. Hollow fibers with a two-dimensionally periodic cladding support air-guided modes of electromagnetic radiation due to the high reflectivity of the cladding within photonic band gaps. Transmission spectra measured for such modes display isolated maxima, visualizing photonic band gaps of the cladding. The spectrum of modes guided by the fibers of this type can be tuned by changing cladding parameters. The possibility of designing hollow photonic-crystal fibers providing maximum transmission for radiation with a desirable wavelength is demonstrated. Fibers designed to transmit 532-, 633-, and 800-nm radiation have been fabricated and tested. The effect of cladding aperiodicity on the properties of modes guided in the hollow core of a microstructure fiber is examined. Hollow fibers with disordered photonic-crystal claddings are shown to guide localized modes of electromagnetic radiation. Hollow-core photonic-crystal fibers created and investigated in this paper offer new solutions for the transmission of ultrashort pulses of high-power laser radiation, improving the efficiency of nonlinear-optical processes, and fiber-optic delivery of high-fluence laser pulses in technological laser systems. *© 2003 MAIK "Nauka/Interperiodica".*

PACS: 42.65.Wi, 42.81.Qb—??

1. INTRODUCTION

Microstructure fibers [1–9] open new horizons in nonlinear optics and spectroscopy, ultrafast optics, optical metrology, and biomedical optics, providing, at the same time, new insights into the basic physical properties of localized modes of electromagnetic radiation in micro- and nanostructured matter. Unique properties of these fibers provide much flexibility for dispersion tailoring [10, 11] and achieving a high confinement degree of light field in the fiber core due to a high refractive-index step between the core and the cladding [12, 13]. A combination of these remarkable opportunities allows many intriguing physical phenomena to be observed and the whole catalogue of nonlinear-optical processes to be enhanced, including the generation of optical harmonics [14, 15] and supercontinuum emission with spectra often spanning more than an octave [16–18], as well as effective parametric interactions [19], four-wave mixing, and stimulated Raman scattering [19, 20] in the field of low-energy laser pulses. Supercontinuum generation is one of the most prominent examples of enhanced nonlinear-optical processes in microstructure and tapered fibers [16–18, 21, 22]. This phenomenon is now changing the paradigm of optical metrology and high-precision measurements [23–25], gaining, at the same time, acceptance in optical coherence tomography [26] and opening new ways for the generation of ultrashort pulses [25] and creation of new sources for spectroscopic applications [18].

Along with conventional waveguiding, supported by total internal reflection, microstructure fibers may, under certain conditions, guide electromagnetic radiation due to the high reflectivity of a periodic fiber cladding within photonic band gaps. Such guided modes can be supported in a hollow core of fibers with a cladding in the form of a two-dimensionally periodic microstructure (two-dimensional photonic crystal). Such fibers, demonstrated for the first time by Cregan *et al.* [26], is one of the most interesting and promising types of microstructure fibers. Photonic band gaps in the transmission of a two-dimensional periodic cladding in these fibers provide high reflection coefficients for electromagnetic radiation propagating along the hollow core of the fiber, allowing a specific regime of

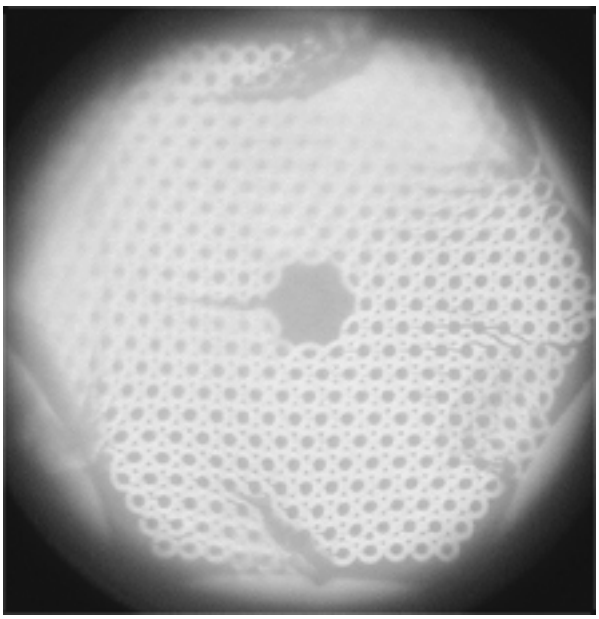

Fig. 1. Cross-sectional image of a microstructure fiber with a two-dimensionally periodic cladding consisting of an array of identical capillaries. This periodic cladding supports guided modes in the hollow core of the fiber due to the high reflectivity of a periodic structure within photonic band gaps. The hollow core of the fiber is formed by removing seven capillaries from the central part of the structure. The period of the structure in the cladding is about 5 μm and the core diameter is about 13 μm.

waveguiding to be implemented [26, 27]. This mechanism of waveguiding is of special interest for telecommunication applications, opening, at the same time, the ways to enhance nonlinear-optical processes, including high-order harmonic generation, in a gas medium filling the fiber core [28]. The possibility of using such fibers for laser manipulation of small-size particles was recently demonstrated by Benabid *et al.* [29].

In this paper, we present the results of our experimental and theoretical investigations of glass fibers with a hollow core and microstructure claddings of different types. We will study hollow fibers with a two-dimensionally periodic cladding, which guide electromagnetic radiation in the hollow core due to the high reflectivity of the cladding within photonic band gaps. The spectrum of air-guided modes localized in the hollow core of our photonic-crystal fibers displays isolated maxima corresponding to photonic band gaps of the cladding. The spectrum of these modes can be tuned by changing cladding parameters. We will explore the effect of cladding aperiodicity on the properties of modes guided in the hollow core of a microstructure fiber and demonstrate that hollow fibers with disordered photonic-crystal claddings can guide localized modes of electromagnetic radiation. The spectrum of such modes still features isolated transmission maxima, but their optical losses are much higher than the optical losses attainable with hollow-core fibers having a photonic-crystal cladding. Hollow-core photonic-crystal fibers created and investigated in this paper offer much promise for telecommunication applications, delivery of high-power laser radiation, laser guiding of atoms and charged particles, as well as high-order harmonic generation and transmission of ultrashort laser pulses.

2. MODELING WAVEGUIDE MODES OF HOLLOW PHOTONIC-CRYSTAL FIBERS: A MODEL OF A PERIODIC COAXIAL WAVEGUIDE AND A FULLY VECTORIAL ANALYSIS

2.1. Model of a Periodic Coaxial Waveguide

For a qualitative analysis of guided modes in hollow-core photonic-crystal fibers (Fig. 1), we employed a model of a coaxial waveguide. Physically, the mechanism behind guided-mode formation in waveguides of this type is similar to the mechanism of waveguiding in hollow-core photonic-crystal fibers, as electromagnetic radiation is confined to the hollow core in both cases due to photonic band gaps of the fiber cladding. The modes of coaxial waveguides have been studied in earlier work [30–34]. In recent years, this effort was, at least partially, motivated by the fabrication and successful demonstration of dielectric coaxial Bragg waveguides [35]. The model of a coaxial waveguide, of course, cannot provide an accurate quantitative description of guided modes in hollow photonic-crystal fibers. However, this model allows the basic features of dispersion properties and transmission spectra of such fibers to be understood in a simple and illustrative way, providing also a general insight into the spatial distribution of electromagnetic radiation in waveguide modes localized in a hollow core of a photonic-crystal fiber.

A two-dimensional periodic structure of the fiber cladding is replaced within the framework of this model by a system of coaxial glass cylinders (see the inset in Fig. 2a) with a thickness b and the inner radius of the ith cylinder equal to

$$r_i = r_0 + i(b + c),$$

where r_0 is the radius of the hollow core and c is the thickness of the gap between the cylinders. Our calculations were performed for coaxial waveguides with an air- or argon-filled hollow core and a cladding consisting of alternating fused silica and air or argon coaxial layers. The data from [36, 37] were used in our calculations to include material dispersion of gases and fused silica.

In a cylindrical system of coordinates $\{r, \varphi, z\}$ with the z-axis directed along the axis of the coaxial waveguide, the longitudinal components of the electric

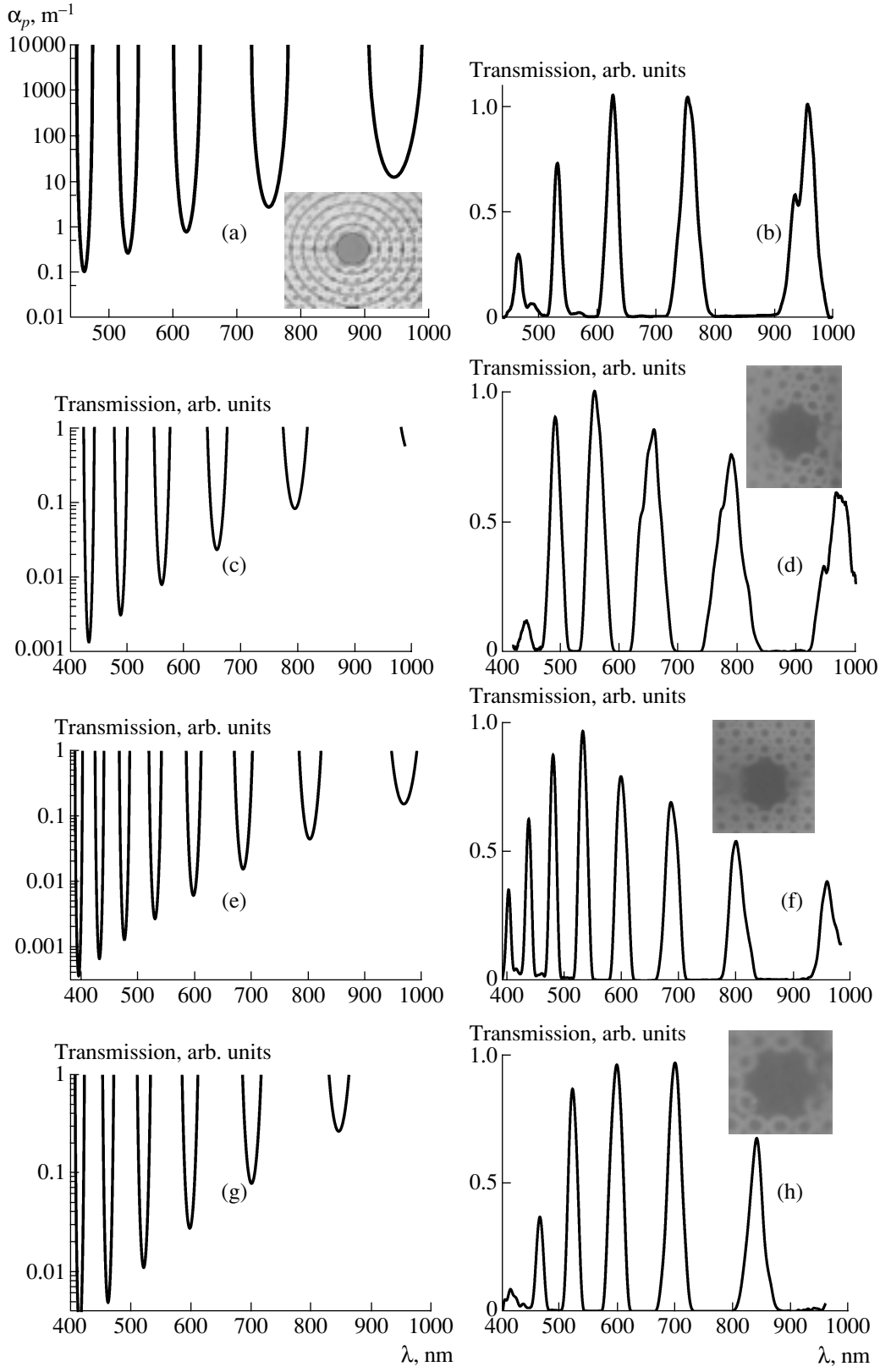

Fig. 2. (a, c, e, g) The attenuation coefficient of the TE_{01} waveguide mode calculated as a function of the wavelength for a periodic coaxial waveguide (see the inset in Fig. 2a) with different parameters: (a) $r_0 = 6.5$ μm, $b = 4.3$ μm, and $c = 0.7$ μm; (c) $r_0 = 7.28$ μm, $b = 4.55$ μm, and $c = 0.95$ μm; (e) $r_0 = 8.6$ μm, $b = 5.55$ μm, and $c = 0.95$ μm; and (g) $r_0 = 7.41$ μm, $b = 4.85$ μm, and $c = 0.75$ μm. (b, d, f, h) Transmission spectra measured for hollow-core photonic-crystal fibers with different cross-section geometries (shown in the insets).

and magnetic fields $E_z(r)$ and $H_z(r)$ in the ith layer of the waveguide are written as [31, 33]

$$E_z(r) = \{A_i J_m(q_i^{(n)} r) + B_i Y_m(q_i^{(n)} r)\}\sin(m\phi + \theta_m), \quad (1)$$

$$H_z(r) = \{C_i J_m(q_i^{(n)} r) + D_i Y_m(q_i^{(n)} r)\}\cos(m\phi + \theta_m), \quad (2)$$

where J_m and Y_m are the Bessel functions of the first and second kind; A_i, B_i, C_i, and D_i are the coefficients determined by boundary conditions; $q_i^{(n)}$ is the transverse part of the propagation constant for the nth waveguide mode; ω is the central frequency of laser radiation; $\beta^{(n)}$ is the propagation constant of the nth mode; m is a nonnegative integer; and θ_m is a real quantity. Transverse components of the electric and magnetic fields can be then calculated in a standard way by substituting Eqs. (1) and (2) into the Maxwell equations (see [33]). Approximate analytical expressions for the electric and magnetic fields in the modes of a coaxial Bragg waveguide have been derived in [31].

We analyzed dispersion properties of modes in a coaxial Bragg waveguide by solving, similar to [33], the characteristic equation derived from the relevant boundary conditions for the tangential components of the electric and magnetic fields at $r = r_i$,

$$T(r_i, \varepsilon_i) = T(r_i, \varepsilon_{i+1})u_{i+1}, \quad (3)$$

where ε_i is the dielectric function of the ith layer,

$$T(r, \varepsilon_i) \equiv \begin{bmatrix} J_m(q_i^{(n)} r) & Y_m(q_i^{(n)} r) & 0 & 0 \\ 0 & 0 & J_m(q_i^{(n)} r) & Y_m(q_i^{(n)} r) \\ \dfrac{jm\beta^{(n)} J_m(q_i^{(n)} r)}{q_i^{(n)^2} r} & \dfrac{jm\beta^{(n)} Y_m(q_i^{(n)} r)}{q_i^{(n)^2} r} & -\dfrac{j\mu_0\beta^{(n)} J_m'(q_i^{(n)} r)}{q_i^{(n)}} & -\dfrac{j\mu_0\beta^{(n)} Y_m'(q_i^{(n)} r)}{q_i^{(n)}} \\ \dfrac{j\varepsilon_i\varepsilon_0\omega J_m'(q_i^{(n)} r)}{q_i^{(n)}} & \dfrac{j\varepsilon_i\varepsilon_0\omega Y_m'(q_i^{(n)} r)}{q_i^{(n)}} & -\dfrac{jm\beta^{(n)} J_m(q_i^{(n)} r)}{q_i^{(n)^2} r} & -\dfrac{jm\beta^{(n)} Y_m(q_i^{(n)} r)}{q_i^{(n)^2} r} \end{bmatrix}, \quad (4)$$

and

$$u_i = [A_i B_i C_i D_i]^t. \quad (5)$$

Geometric parameters of the layers forming the coaxial waveguide were chosen in such a way as to achieve the air-filling fraction of the fiber cladding measured in our experiments. In particular, for the photonic-crystal fiber with the cross section shown in Fig. 1, the period of the photonic-crystal cladding is $\Lambda \approx 5$ μm and the diameter of holes in the cladding is $a \approx 2.1$ μm. The air-filling fraction of the fiber cladding can then be estimated as

$$\eta = \frac{\pi a^2}{4\Lambda^2} \approx 14\%.$$

This estimate on the air-filling fraction of the fiber cladding dictates the following parameters of the coaxial waveguide: $b \approx 4.3$ μm and $c \approx 0.7$ μm. Figures 2a, 2c, and 2e present the results of calculations performed for hollow photonic-crystal fibers with different sizes of air holes and different air-filling fractions of the cladding. As far as the central frequencies and bandwidths of transmission peaks are concerned, predictions of this simple model agree qualitatively well with the experimental transmission spectra measured for these fibers and presented in Figs. 2b, 2d, and 2f.

To estimate the magnitude of optical losses for the modes of a coaxial periodic waveguide, we will employ the following simple arguments. Let us write the coefficient of reflection R of the electric field from the periodic structure of the fiber cladding in terms of the notations introduced above:

$$R = 1 - \frac{(A_N)^2 + (B_N)^2}{(A_0)^2 + (B_0)^2}. \quad (6)$$

Introducing the angle φ between the direction of ray trajectory representing the waveguide mode in the fiber core and the z-axis, we can express the distance between the points of two successive beam reflections (the half-period of the ray trajectory) as

$$L_p = \frac{2a}{\tan\varphi}. \quad (7)$$

The number of reflections within a fiber section with a length equal to the attenuation length $L_\alpha = 1/\alpha$ (where L_α is the magnitude of optical losses) is given by

$$N_r = \frac{L_\alpha}{2L_p}. \quad (8)$$

The magnitude of optical losses then meets the relation

$$R^{N_r} = \exp(-\alpha L_\alpha). \quad (9)$$

Keeping in mind that

$$\tan\varphi = \frac{(u^{(n)}/\alpha)}{\beta^{(n)}} = \frac{q_0^{(n)}}{\beta^{(n)}} = \frac{(k^2\varepsilon_1 - (\beta^{(n)})^2)^{1/2}}{\beta^{(n)}},$$

and using Eqs. (6)–(9), we finally arrive at the following expression for the magnitude of losses of the electric field in a hollow-core periodic coaxial waveguide:

$$\alpha = -\frac{\ln R}{2L_p} = -\frac{\ln\left(1 - \frac{(A_N)^2 + (B_N)^2}{(A_0)^2 + (B_0)^2}\right)(k^2\varepsilon_1 - (\beta^{(n)})^2)^{1/2}}{4\alpha\beta^{(n)}}. \quad (10)$$

Figure 2c displays the results of calculations performed for a hollow periodic coaxial waveguide whose cladding parameters are chosen in such a way as to achieve maximum transmission at the wavelength of 0.8 μm. The period of the cladding in such a waveguide is $b + c = 5.5$ μm, the thickness of the fused silica layer is $b = 4.55$ μm, and the core radius is 7.28 μm. Figure 2d presents the results of experimental measurements carried out on a fiber with the cross-section structure shown in the inset to this figure. Comparison of these plots shows a satisfactory qualitative agreement between the results of calculations and the experimental data. Transmission spectra of photonic-crystal fibers display isolated peaks, which have been earlier observed also in experiments [26, 27]. No localized guided modes may exist outside these frequency ranges. The finite widths of transmission peaks limit the bandwidths and, consequently, the duration of laser pulses that can be transmitted with minimal losses through photonic-crystal waveguides. As shown in [38], laser pulses with durations on the order of tens of femtoseconds can still be transmitted through hollow-core photonic-crystal fibers as localized air-guided modes.

2.2. Fully Vectorial Analysis

Predictions of the model of a periodic coaxial waveguide qualitatively agree with the results of more accurate, but much more complicated, fully vectorial analysis of modes in a hollow photonic-crystal fiber. We performed such an analysis using the approach proposed by Monro *et al.* [39] and based on the numerical solution of the eigenfunction and eigenvalue problem corresponding to the vectorial Maxwell equation for the electric field $\mathbf{E}(z, t) = \mathbf{E}\exp(i(\beta z - ckt))$, $\mathbf{E} = (E_x, E_y, E_z)$:

$$\left[\frac{\nabla^2}{k^2} + n^2\right]E_n + \frac{1}{k^2}\frac{\partial}{\partial y} \times \left(E_x\frac{\partial \ln(n^2)}{\partial x} + E_y\frac{\partial \ln(n^2)}{\partial y}\right) = \frac{\beta^2}{k^2}E_x, \quad (11)$$

$$\left[\frac{\nabla^2}{k^2} + n^2\right]E_y + \frac{1}{k^2}\frac{\partial}{\partial y} \times \left(E_x\frac{\partial \ln(n^2)}{\partial x} + E_y\frac{\partial \ln(n^2)}{\partial y}\right) = \frac{\beta^2}{k^2}E_y, \quad (12)$$

where β is the propagation constant, k is the wave number, ∇ is the gradient operator, and $n(x, y)$ is the two-dimensional profile of the refractive index.

Transverse distribution of the electric field in the cross section of the fiber is represented as an expansion in orthonormalized Hermite–Gauss functions:

$$E_x = \sum_{n,m=0}^{F-1} \xi_{n,m}^x \psi_n\left(\frac{x}{\Lambda}\right)\psi_m\left(\frac{y}{\Lambda}\right),$$
$$E_y = \sum_{n,m=0}^{F-1} \xi_{n,m}^y \psi_n\left(\frac{x}{\Lambda}\right)\psi_m\left(\frac{y}{\Lambda}\right). \quad (13)$$

The profile of the refractive index squared, $n^2(x, y)$, is also represented as an expansion in Hermite–Gauss functions and a set of orthogonal periodic functions (cosine functions in our case). Substituting these functional series into the wave equations reduces our vectorial problem to an eigenfunction and eigenvalue problem for the relevant matrix equation. Solving this problem, we can find the propagation constants and spatial field distributions in waveguide modes.

Figures 3a and 3b present transverse field intensity distributions calculated with the use of the above-described approach for a hollow-core photonic-crystal fiber with the cross-section structure similar to that shown in Fig. 1 around the maximum-transmission frequency in the visible spectral range. Transverse field intensity distributions shown in Figs. 3a and 3b correspond to the fundamental and higher order modes guided in the hollow photonic-crystal fiber, respectively. Thus, our vectorial numerical analysis also indicates the existence of higher order air-guided modes localized under the above-specified conditions in the hollow core of a photonic-crystal fiber.

We have demonstrated that the predictions of the model of a coaxial periodic waveguide provide a satisfactory qualitative agreement with the results of the vectorial analysis of guided modes in a hollow photo-

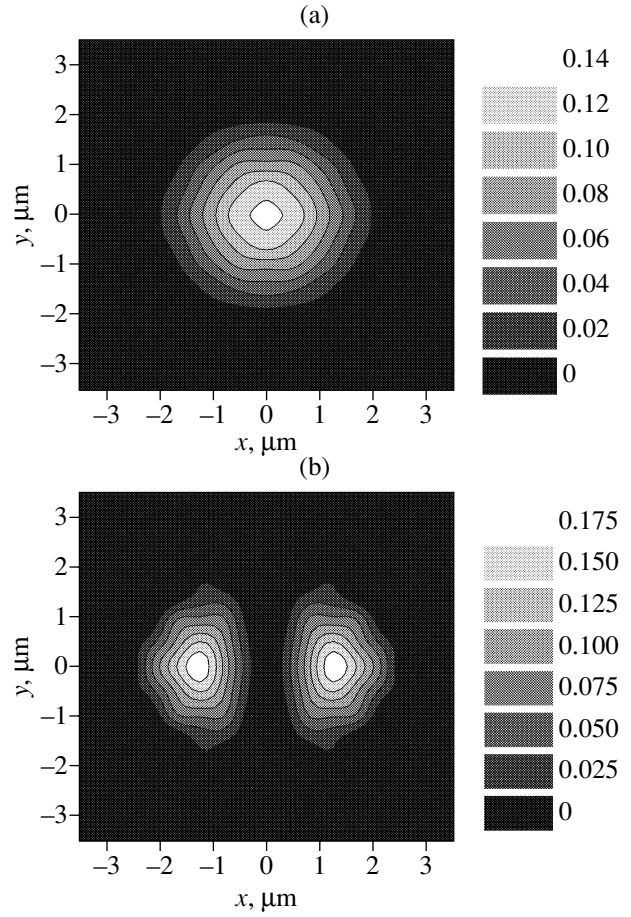

Fig. 3. Transverse radiation intensity distribution in (a) the fundamental and (b) higher order air-guided modes calculated by means of vectorial analysis of electromagnetic field in a photonic-crystal fiber with the cross-section structure similar to that shown in Fig. 1.

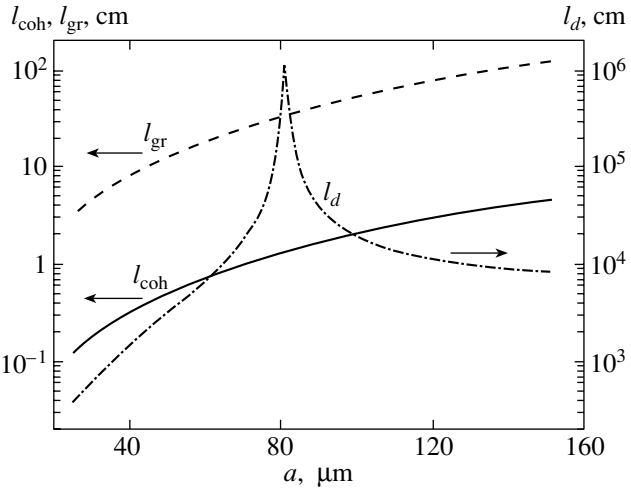

Fig. 4. Dispersion spreading length l_d for 35-fs pulses of 800-nm radiation calculated as a function of the inner radius of a hollow fiber a for the fundamental EH_{11} mode. Coherence length for mode cross-talk l_{coh} and the walk-off length l_{gr} are also shown. The hollow core of the fiber is filled with argon at the pressure of 1 atm.

nic-crystal fiber, as well as with the results of experimental studies (see Section 4). This finding allows us to suggest the model of a hollow coaxial waveguide as a simple framework for elementary estimates of dispersion parameters and qualitative understanding of the spatial distribution of electromagnetic radiation in the guided modes of hollow-core photonic-crystal fibers.

2.3. Group-Velocity Dispersion and Transmission of Ultrashort Pulses

Guided modes of hollow photonic-crystal fibers are ideally suited for the transmission and control of ultrashort light pulses. Due to the fact that the group-velocity dispersion of gases filling a hollow core of photonic-crystal fibers is much lower than the group-velocity dispersion typical of dielectric materials used in standard fibers, temporal spreading of short light pulses transmitted by air-guided modes of hollow-core photonic-crystal fibers is much less critical than in the case of guided modes of standard fibers. This important circumstance, however, by no means exhausts the benefits offered by hollow-core photonic-crystal fibers for the transmission and control of ultrashort pulses of electromagnetic radiation. Aside from the material of the fiber, dispersion properties of guided modes in hollow photonic-crystal fibers are sensitive to the core–cladding geometry. This circumstance allows dispersion tailoring by changing the fiber structure. In the case of microstructure fibers with a dielectric core, which guide electromagnetic radiation by total internal reflection, flat group-velocity dispersion profiles can be shaped, with the sign and the absolute value of group-velocity dispersion controlled by varying the period of the structure, the air-filling fraction of the cladding, and filling the air holes in the cladding with different materials [12, 13]. Similar efficient solutions for hollow-core photonic-crystal fibers are still to be found. The results of our experimental studies presented in Section 4 demonstrate that the transmission spectrum and, consequently, the dispersion of hollow photonic-crystal fibers can be tuned by changing the structure of the fiber cladding. Numerical simulations [38] reveal the regions of low group-velocity dispersion within transmission peaks of these fibers.

Away from the edges of photonic band gaps of a periodic fiber cladding, the frequency dependence of group-velocity dispersion of modes guided in the hollow core of a photonic-crystal fiber is similar to the spectral dependence of group-velocity dispersion for a metal hollow fiber [34]. We can, therefore, employ several useful relations known from the theory of solid-cladding hollow fibers to assess the dependence of the group-velocity dispersion of guided modes in hollow photonic-crystal fibers on parameters of such fibers far from the edges of photonic band gaps. In particular, the

group-velocity dispersion D scales as approximately the inverse square of the inner fiber diameter a,

$$D \sim -a^{-2}$$

[34]. The increase in the inner fiber radius thus allows the effects related to the dispersion spreading of ultrashort pulses to be reduced. Figure 4 shows the dispersion length for 35-fs pulses of 800-nm radiation propagating in an argon-filled hollow fiber as a function of the inner radius of this fiber. As can be seen from this dependence, zero group-velocity dispersion is achieved with an inner fiber radius equal to 80 μm.

Figure 5 displays the dependences of the group index and group-velocity dispersion on the wavelength for a hollow fiber with an inner radius of 68 μm filled with molecular hydrogen at a pressure of 0.5 atm. Group-velocity dispersion under these conditions is low within the entire spectral range under study, vanishing at the wavelength of 560 nm (see also [40]). Importantly, for long wavelengths, dispersion properties of guided modes are mainly determined by the waveguide dispersion component, while for short wavelengths, the material dispersion of the gas filling the fiber plays the dominant role. The group velocity and group-velocity dispersion as functions of the wavelength asymptotically tend in these limiting cases (Fig. 5) to the dependences characteristic of the waveguide (dotted lines) and material (dashed lines) dispersion components.

Hollow coaxial Bragg waveguides with a small inner radius, on the other hand, allow high absolute values of group-velocity dispersion to be achieved, providing an opportunity to compensate for strong material dispersion of gases filling the fiber core [41]. Reflection from the periodic structure of a fiber cladding is accompanied by an additional phase shift [42], modifying the frequency dependence of group-velocity dispersion and making the spectral dependences of dispersion parameters of hollow coaxial Bragg waveguides and photonic-crystal fibers deviate from the approximate dependences characteristic of guided modes in metal hollow waveguides.

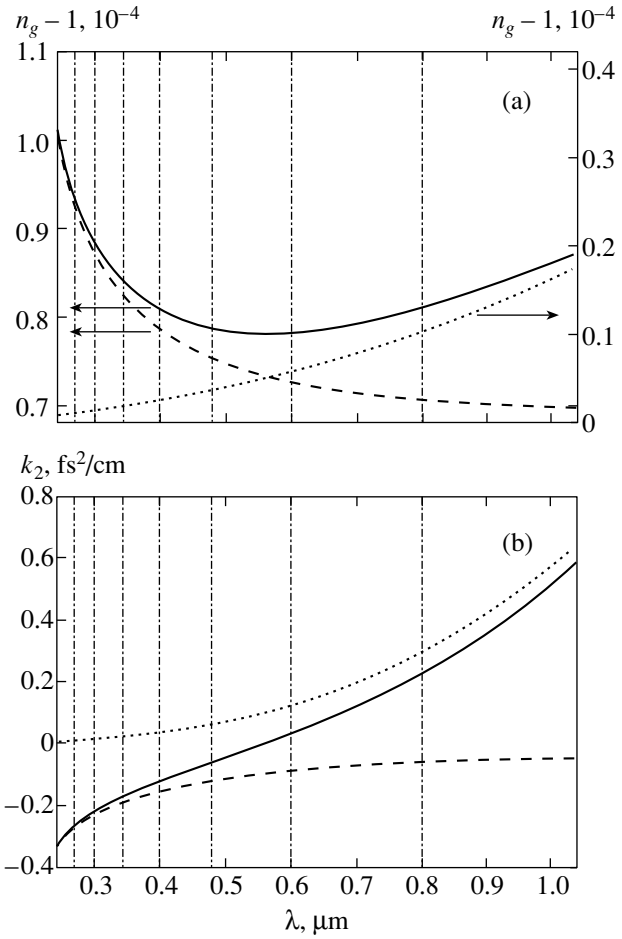

Fig. 5. (a) The group index $n_g = c/v_g$ and (b) group-velocity dispersion calculated as functions of the wavelength (dashed lines) for molecular hydrogen, (dotted lines) the EH_{11} waveguide mode, and (solid lines) the EH_{11} mode of a hollow fiber filled with molecular hydrogen. The gas pressure is 0.5 atm. The inner radius of the fiber is 68 μm. The vertical lines show Raman sidebands produced through the stimulated Raman scattering of the second harmonic of a Ti: sapphire laser.

3. EXPERIMENTAL

Hollow microstructure fibers with a two-dimensionally periodic (photonic-crystal) cladding were fabricated with the use of a preform consisting of a set of identical glass capillaries. Seven capillaries were removed from the central part of the preform for the hollow core of photonic-crystal fibers. The cross-section image of a fiber fabricated by drawing such a preform is presented in Fig. 1. A typical period of the structure in the cladding of the fiber shown in Fig. 1 is about 5 μm. The diameter of the hollow core of the fiber is then approximately equal to 13 μm. Varying the period of the photonic-crystal structure in the fiber cladding and changing its air-filling fraction, we were able to tune the transmission spectrum of air-guided modes, providing optimal conditions for a waveguide transmission of radiation with different wavelengths (see Section 4). The length of fiber samples employed in our experiments ranged from several centimeters up to 1 m.

Special microstructure fibers have been designed and fabricated to investigate the effect of fiber-cladding aperiodicity on the properties of guided modes. These fibers had an aperiodic cladding, characterized by the presence of short-range order (Fig. 6). A preform with a larger central capillary surrounded with smaller capillaries was employed to fabricate such fibers. The cobweb structure of the cladding in such a fiber, as can be seen from Fig. 6, features, in a certain approximation, a short-range order in the arrangement of glass channels linked by narrow bridges. The fiber cross-section image shown in Fig. 6 also visualizes a set of roughly concentric glass rings, surrounding the fiber core, with a fuzz-

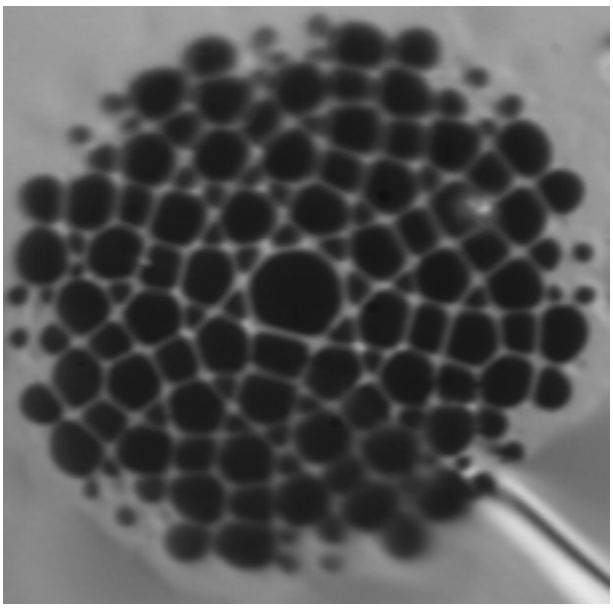

Fig. 6. A cross-sectional microscopic image of a cobweb fiber with a disordered microstructure cladding. The ring system of glass channels at the center of this fiber forms a two-dimensional photonic molecule. The distance between the neighboring channels is 7.4 μm.

ily defined characteristic spacing between them. Air-
2 filled holes, arranged aperiodically in the fiber cladding, and the larger hole at the center of the fiber form an array of small-diameter glass waveguides linked with thin bridges around the central hole (Fig. 6). Such a microstructure-integrated bundle of fibers provides a high degree of light confinement due to the total internal reflection from the high-refractive-index-step glass–air interface. Dispersion aspects of pulse propagation and nonlinear-optical interactions in such fiber structures can be controlled by exciting different combinations of collective waveguide modes.

The central ring array of waveguides in the considered cobweb fiber is reminiscent in its structure of a cyclic polyatomic molecule consisting of identical atoms (Fig. 6). As shown earlier [43, 44], the properties of guided modes in such a ring array of coupled waveguides are similar to the properties of electron wave functions in a two-dimensional polyatomic cyclic molecule. The basic dispersion properties of guided modes in this coupled-waveguide array can be described in a convenient and illustrative way in terms of the photonic-molecule model. The high degree of light localization in these photonic-molecule modes of a cobweb microstructure fiber provides a high efficiency of nonlinear-optical interactions, allowing octave spectral broadening to be achieved with low-energy femtosecond pulses. The results of experimental studies presented in Section 4.2 of this paper demonstrate that this microstructure fiber not only guides electromagnetic radiation through the central array of microstructure-integrated waveguides, but also supports air-guided modes in its hollow core. Our studies of hollow microstructure fibers with periodic and aperiodic claddings performed in this paper allow the influence of cladding aperiodicity and disorder on the properties of air-guided modes in microstructure fibers to be assessed, providing a deeper insight into the physics of such modes, as well as the fundamental aspects of light propagation and scattering in photonic band-gap structures.

4. RESULTS AND DISCUSSION

4.1. Hollow Photonic-Crystal Fibers

The idea of lowering the magnitude of optical losses in a hollow fiber with a periodically microstructured cladding relative to the magnitude of optical losses in a hollow fiber with a solid cladding is based on the high reflectivity of a periodic structure within photonic band gaps [45]. In hollow fibers, the refractive index of the core is lower than the refractive index of the cladding. Therefore, the propagation constants of hollow-fiber modes have nonzero imaginary parts, and the propagation of light in such fibers is accompanied by radiation losses. The magnitude of optical losses in hollow fibers scales [46] as λ^2/a^3, where λ is the radiation wavelength and a is the inner radius of the fiber. Such a behavior of the magnitude of optical losses prevents one from using hollow fibers with very small inner diameters in nonlinear-optical experiments [42, 47]. Our estimates show that the magnitude of radiation losses for the fundamental mode of a hollow fiber with a fused silica cladding and an inner radius of 6.5 μm may reach 20 cm^{-1} for 0.8-μm radiation, which, of course, imposes serious limitations on applications of such fibers. Radiation losses can be radically reduced in the case of hollow fibers with a periodic cladding.

Our experimental studies confirm the possibility of using hollow photonic-crystal fibers with a core diameter of about 13 μm to guide coherent and incoherent radiation. Figure 7 displays the spatial distributions of intensity of incoherent (Fig. 7a) and coherent (Fig. 7b) radiation obtained by imaging the output end of a hollow photonic-crystal fiber with the above-specified parameters. Optimizing the geometry of coupling of laser radiation into the fiber, we were able to achieve a high degree of light-field confinement in the hollow core of the fiber without losing too much energy through mode excitation in the photonic-crystal cladding (Fig. 7a). The spatial distribution of radiation intensity at the output end of the fiber under these conditions corresponded to the fundamental waveguide mode.

To investigate the spectrum of modes guided in the hollow core of photonic-crystal fibers, we used a diaphragm to separate radiation transmitted through the hollow core from radiation guided by the cladding. The spectra of modes supported by the hollow core of pho-

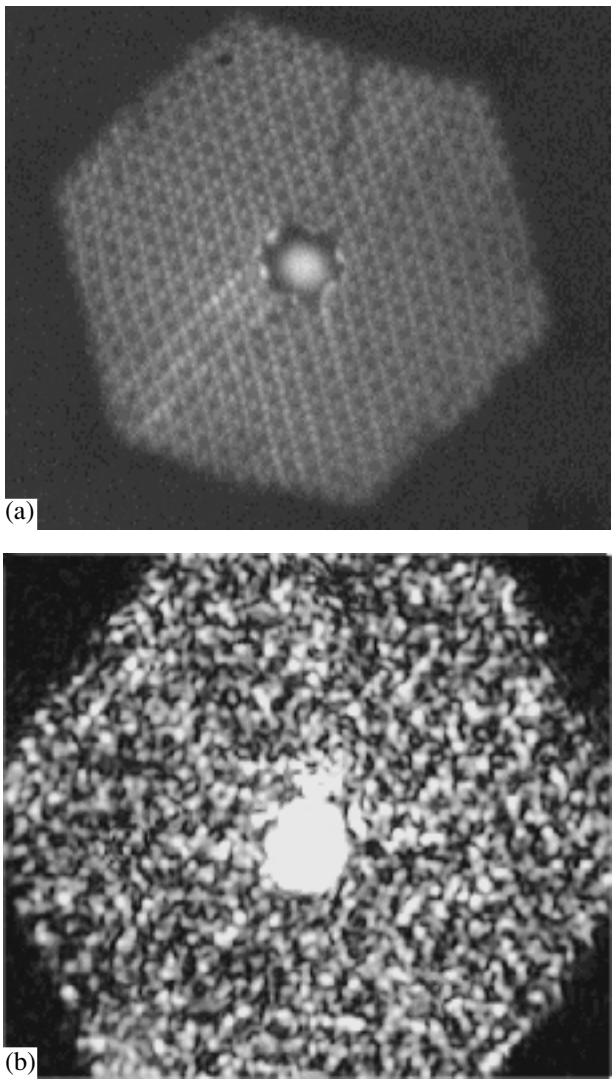

Fig. 7. Radiation intensity distribution in the cross section of a hollow photonic-crystal fiber with a period of the structure in the cladding of about 5 μm and the core diameter of approximately 13 μm. (a) A waveguide mode is excited in the hollow core with a broad beam of incoherent light. (b) The fundamental waveguide mode of the hollow core is excited with 633-nm diode-laser radiation.

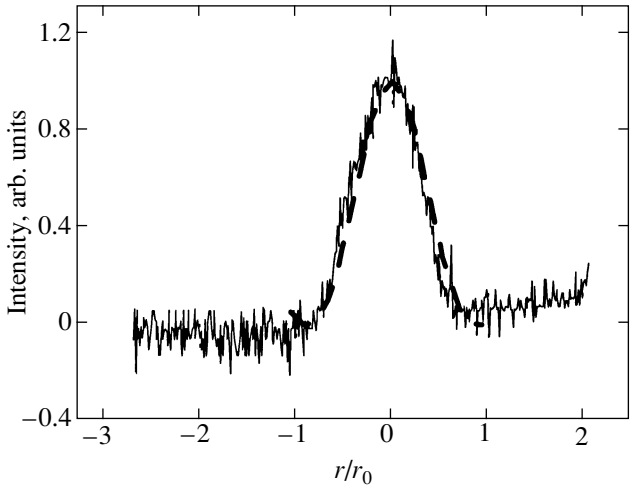

Fig. 8. Transverse intensity distribution of electromagnetic radiation (solid line) measured at the output of a hollow-core photonic-crystal fiber and (dashed line) calculated with the use of the model of a periodic coaxial waveguide.

tonic-crystal fibers were measured within the range of wavelengths from 450 up to 1000 nm. These spectra displayed characteristic well-pronounced isolated peaks (Figs. 2b, 2d, 2f, 2h). Similar peaks in transmission spectra of hollow photonic-crystal fibers have been also observed in earlier work [26, 27]. The origin of these peaks is associated with the high reflectivity of a periodically structured fiber cladding within photonic band gaps, which substantially reduces radiation losses in guided modes within narrow spectral ranges. Radiation with wavelengths lying away from photonic band gaps of the cladding leaks from the hollow core. Such leaky radiation modes are characterized by high losses, giving virtually no contribution to the signal at the output of the fiber. The spectra of air-guided modes in hollow photonic-crystal fibers were tuned by changing the fiber cladding structure. In Figs. 2a–2h, this tunability option is illustrated by transmission spectra 3 measured for hollow photonic-crystal fibers with different cross-section structures (shown in the insets to Figs. 2a, 2d, 2f, 2h).

As can be seen from the comparison of the results of calculations (Figs. 2a, 2c, 2e, 2g), carried out with the use of the approach described in Section 2.1, with the experimental data shown in Figs. 2b, 2d, 2f, 2h, the model of a periodic coaxial waveguide provides qualitatively adequate predictions for the positions and the widths of spectral bands where the hollow core of a photonic-crystal fiber can guide electromagnetic radiation with minimum losses. Variations in the structure of the photonic-crystal cladding were modeled with our approach by accommodating the thicknesses of coaxial layers constituting the Bragg waveguide in such a way as to achieve the required air-filling fraction of the photonic-crystal fiber. This approach allowed us to design hollow photonic-crystal fibers providing maximum transmission for a given wavelength. In particular, fibers with the cross-section structure shown in the insets to Figs. 2d and 2f feature transmission peaks at the wavelength of 800 nm and can be employed to transmit Ti: sapphire laser radiation. Fibers with the cross-section structure presented in the insets to Figs. 2f and 2h display transmission peaks at 532 nm, offering the way to transport second-harmonic radiation of a neodymium garnet laser.

The model of a periodic coaxial waveguide, as can be seen from Figs. 8 and 9, also gives a satisfactory qualitative description for radiation intensity distributions in the fundamental (Fig. 8) and higher order (Fig. 9) waveguide modes of a photonic-crystal fiber.

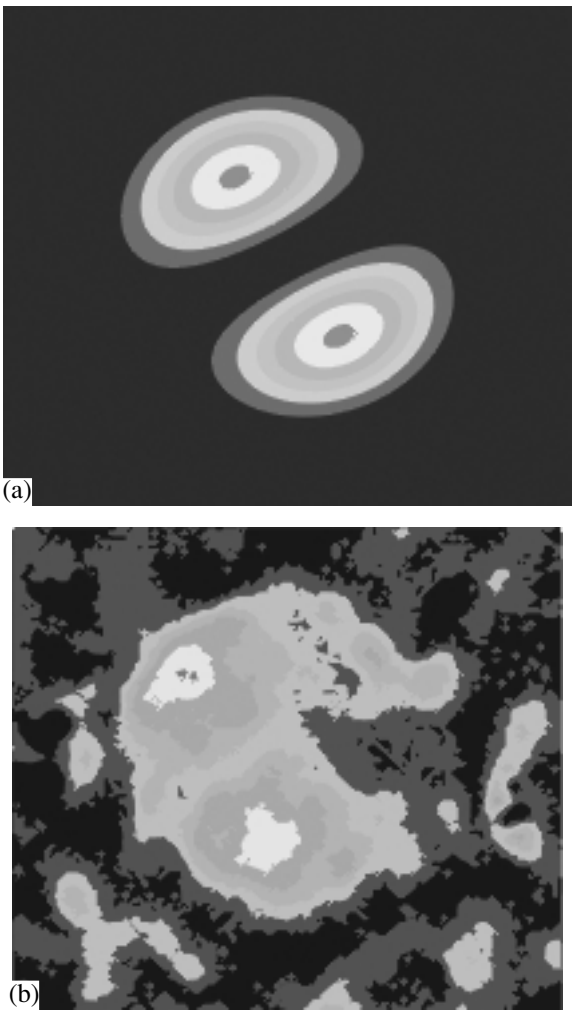

Fig. 9. (a) Transverse distribution of the electric field squared in a higher order mode of a hollow-core photonic-crystal fiber calculated with the use of the model of a periodic coaxial waveguide. (b) Transverse intensity distribution of electromagnetic radiation measured at the output of a hollow-core photonic-crystal fiber with a higher order waveguide mode of the fiber excited with 633-nm radiation of a diode laser.

Comparison of Figs. 3, 7–9 allows a judgement of the qualitative agreement between the experimental data, theoretical predictions obtained with the model of a periodic coaxial waveguide, and the results of a more accurate, but more complicated vectorial analysis of guided modes in a hollow photonic-crystal fiber (see Section 2.2).

The spatial distribution of 633-nm diode-laser radiation (this wavelength falls within one of the transmission peaks in Figs. 2a, 2b, corresponding to the guided modes of the photonic-crystal fiber) at the output of an 8-cm hollow photonic-crystal fiber indicates the existence of multimode regimes of waveguiding around this wavelength. As shown in [28], multimode waveguiding regimes in hollow photonic-crystal fibers can be

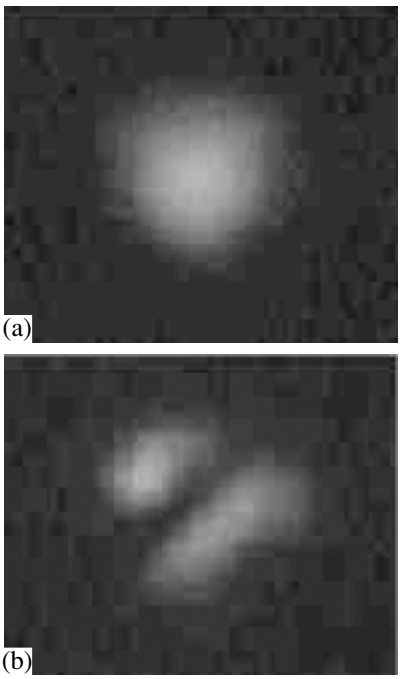

Fig. 10. Transverse intensity distributions of 1.06-μm laser radiation at the output of a hollow-core photonic-crystal fiber (a) in the fundamental and (b) in the higher order waveguide modes.

employed to enhance high-order harmonic generation in nonlinear gases filling the hollow cores of these fibers. The waveguide contribution to the mismatch of propagation constants related to the guided modes of the pump and harmonic radiation increases with a decrease in the core diameter of a hollow fiber [48]. Our photonic-crystal fiber with a small core diameter is, therefore, characterized by a strong dispersion of guided modes, allowing considerable phase mismatches related to the material dispersion of nonlinear gases to be compensated. This efficient phase-mismatch compensation becomes possible due to the unique properties of hollow photonic-crystal fibers, as the leaky modes guided in hollow fibers with a solid cladding and a diameter of the hollow core of about 13 μm would have, as mentioned above, unacceptably high losses.

The possibility of transporting high-power laser pulses through hollow-core photonic-crystal fibers was demonstrated by our experiments with 40-ps neodymium garnet laser pulse trains with a total energy of 1 mJ transmitted through a hollow photonic-crystal fiber with an inner diameter of 13 μm. The energy fluence of laser energy in these experiments reached 100 J/cm^2, which was an order of magnitude higher than the optical breakdown threshold for fused silica. A hollow photonic-crystal fiber allowed sequences of picosecond laser pulses to be transmitted in both single-mode (Fig. 10a) and multimode (Fig. 10b) regimes, providing laser fluences and spatial beam quality at the

output of the fiber sufficient to initiate optical breakdown on different targets.

4.2. Hollow Fibers with an Aperiodic Microstructure Cladding

To examine the effect of disorder and aperiodicity of the cladding structure on the properties of guided modes and waveguiding regimes in hollow-core photonic-crystal fibers, we investigated the spectrum of modes supported in the hollow core of microstructure fibers with an aperiodic cladding featuring a short-range order of the cladding structure (Fig. 6). As shown in earlier work [43, 44], a structure consisting of seven linked glass channels in the central part of the cross section of such fibers and surrounding the hollow fiber core guides localized modes of electromagnetic radiation, which are classified as photonic-molecule modes. Our experiments have shown that the fibers of this type may also transmit light through guided modes localized in their hollow core. Figure 11a presents the spectrum of radiation transmitted through the hollow core of such fibers. To measure this spectrum, we selected radiation guided through the hollow core from radiation transmitted through the thin ring glass (photonic-molecule) structure surrounding the hollow core with the use of a diaphragm. In spite of the aperiodicity of the fiber cladding, clearly pronounced transmission peaks are observed in the spectra of radiation transmitted through the hollow core of the fiber. The spectra of radiation transmitted through the thin ring glass structure surrounding the hollow core are continuous, indicating different physics of waveguiding and giving rise to a pedestal in the spectra measured with a diaphragm adjusted to select radiation transmitted through the central part of the fiber, including the hollow core and the photonic-molecule part of the cladding (Fig. 11b).

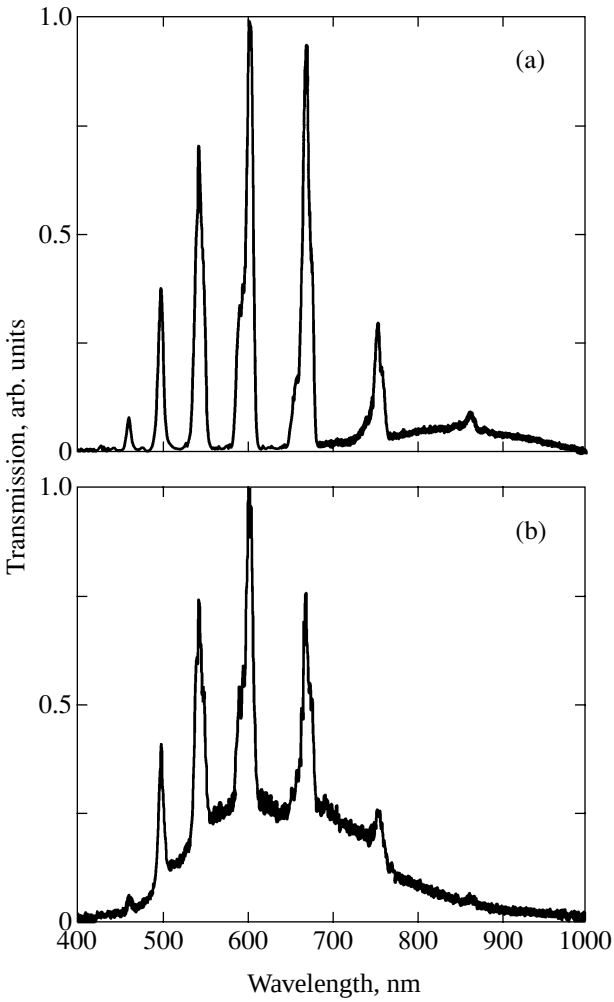

Fig. 11. Transmission spectra of a hollow fiber with a disordered microstructure cladding measured (a) with a diaphragm set to select radiation transmitted through the hollow core of the fiber and (b) with a diaphragm selecting radiation transmitted through the hollow core and the ring glass photonic-molecule structure in the central part of the fiber (Fig. 6).

One practical aspect revealed by these studies is that waveguiding in a hollow core of photonic-crystal fibers involves some tolerances on deviations from the ideal periodicity of the cladding. The results of these experiments also provide deeper insights into the basic physical issues related to the origin of photonic band gaps and waveguide modes in hollow photonic-crystal and microstructure fibers, as well as regimes of light scattering and interference in disordered and amorphous photonic crystals [49–54]. Our experiments demonstrate, in particular, that air-guided modes in hollow microstructure fibers can be supported, in particular, due to reflection from a cladding with a short-range order. The cladding of microstructure fibers employed in these experiments features, in some approximation, two types of spatial regularity—a short-range order, similar to that typical of amorphous photonic crystals, and the existence of some fuzzily defined characteristic separation between concentric rings in the cladding structure (see Fig. 6).

Localized air-guided modes in hollow photonic-crystal fibers with an ideally periodic cladding are associated with the existence of photonic band gaps in the transmission of the cladding. Within these frequency ranges, electromagnetic radiation cannot leak from the core into the cladding of a fiber. Evanescent fields existing in the photonic-crystal fiber cladding within the photonic band gaps rapidly decay with the growth in the distance from the fiber core. As some disorder is introduced into the fiber cladding, allowed states arise within the photonic band gap. The density of such states increases as the degree of structure disorder grows [54]. Allowed states in the photonic band gap may substantially modify transmission spectra of hollow microstructure fibers. The modes guided along the hollow core of such fibers become more and more lossy, leaking into the cladding as the density of allowed states grows within the photonic band gap of the fiber cladding. The spectrum presented in Fig. 11a

corresponds to an intermediate regime when the density of allowed states, arising within the photonic band gaps due to the aperiodicity and disorder of the microstructure cladding, is still low, permitting the existence of localized air-guided modes in the hollow core of the fiber.

5. CONCLUSION

Experimental and theoretical studies presented in this paper reveal several important properties of modes guided by hollow-core microstructure fibers with two-dimensionally periodic and aperiodic claddings. We have also demonstrated that such fibers offer new solutions for the transmission of ultrashort pulses of high-power laser radiation, improving the efficiency of nonlinear-optical processes, and fiber-optic delivery of high-fluence laser pulses in technological laser systems. Hollow photonic-crystal fibers support air-guided modes of electromagnetic radiation localized in the hollow core due to the high reflectivity of the fiber cladding within photonic band gaps. Experimentally measured spectra of such modes display isolated maxima corresponding to photonic band gaps of the photonic-crystal cladding. The manifolds of such transmission peaks can be tuned by changing cladding parameters. The effect of cladding aperiodicity on the properties of modes guided in the hollow core of a microstructure fiber was analyzed. We have shown the possibility of designing hollow photonic-crystal fibers providing maximum transmission for radiation with a desirable wavelength. Hollow photonic-crystal fibers designed to transmit 532-, 633-, and 800-nm radiation have been fabricated and tested.

Our experiments also demonstrate the existence of localized air-guided modes of electromagnetic radiation in hollow fibers with disordered and aperiodic microstructure claddings. The spectra of such modes still feature isolated transmission maxima, but their optical losses are much higher than the optical losses attainable with hollow-core fibers having a photonic-crystal cladding. From the technological viewpoint, this implies that requirements to the periodicity of the photonic-crystal fiber cladding can be loosened under certain conditions. Fundamental aspects of these studies involve using isolated transmission peaks observed for hollow microstructure fibers with an aperiodic cladding as a clue to getting a deeper insight into the formation of photonic band gaps and regions of low photonic densities of states and, more generally, understanding regimes of light scattering and interference in random and amorphous photonic crystals.

Hollow-core photonic-crystal fibers created and investigated in this paper offer new solutions to many problems of basic physics and applied optics. Such fibers hold much promise, in particular, for telecommunication applications and delivery of high-power laser radiation. Due to their remarkable properties, these fibers offer a unique opportunity of implementing nonlinear-optical interactions of waveguide modes with transverse sizes of several microns in a gas medium, opening the ways to improve the efficiency of optical frequency conversion for ultrashort pulses and enhance high-order harmonic generation. The spectra of air-guided modes in hollow-core photonic-crystal fibers, featuring isolated transmission peaks, are ideally suited for wave-mixing spectroscopic applications and frequency conversion through stimulated Raman scattering. Further exciting applications of these fibers include generation and guiding of ultrashort pulses, extendable to subfemtosecond x-ray field waveforms, manipulation of atoms and charged particles, and creation of highly sensitive gas sensors.

ACKNOWLEDGMENTS

This study was supported in part by the President of Russian Federation Grant no. 00-15-99304, the Russian Foundation for Basic Research (projects nos. 00-02-17567 and 02-02-17098), the Volkswagen Foundation (project I/76 869), and the European Research Office of the US Army (contract no. N62558-02-M-6023).

REFERENCES

1. J. C. Knight, T. A. Birks, P. St. J. Russell, and D. M. Atkin, Opt. Lett. **21**, 1547 (1996).
2. J. C. Knight, J. Broeng, T. A. Birks, and P. St. J. Russell, Science **282**, 1476 (1998).
3. Opt. Express **9** (13) (2001), Focus Issue, Ed. by K. W. Koch.
4. J. Opt. Soc. Am. B **19** (2002), Special Issue, Ed. by C. M. Bowden and A. M. Zheltikov.
5. T. M. Monro, P. J. Bennett, N. G. R. Broderick, and D. J. Richardson, Opt. Lett. **25**, 206 (2000).
6. A. B. Fedotov, A. M. Zheltikov, L. A. Mel'nikov, *et al.*, Pis'ma Zh. Éksp. Teor. Fiz. **71**, 407 (2000) [JETP Lett. **71**, 281 (2000)]; M. V. Alfimov, A. M. Zheltikov, A. A. Ivanov, *et al.*, Pis'ma Zh. Éksp. Teor. Fiz. **71**, 714 (2000) [JETP Lett. **71**, 489 (2000)].
7. A. M. Zheltikov, Usp. Fiz. Nauk **170**, 1203 (2000) [Phys.–Usp. **43**, 1125 (2000)].
8. A. M. Zheltikov, M. V. Alfimov, A. B. Fedotov, *et al.*, Zh. Éksp. Teor. Fiz. **120**, 570 (2001) [JETP **93**, 499 (2001)].
9. B. J. Eggleton, C. Kerbage, P. S. Westbrook, *et al.*, Opt. Express **9**, 698 (2001).
10. N. G. R. Broderick, T. M. Monro, P. J. Bennett, and D. J. Richardson, Opt. Lett. **24**, 1395 (1999).
11. A. B. Fedotov, A. M. Zheltikov, A. P. Tarasevitch, and D. von der Linde, Appl. Phys. B **73**, 181 (2001).
12. J. C. Knight, J. Arriaga, T. A. Birks, *et al.*, IEEE Photonics Technol. Lett. **12**, 807 (2000).
13. W. H. Reeves, J. C. Knight, P. St. J. Russell, and P. J. Roberts, Opt. Express **10**, 609 (2002).
14. J. K. Ranka, R. S. Windeler, and A. J. Stentz, Opt. Lett. **25**, 796 (2000).
15. A. N. Naumov, A. B. Fedotov, A. M. Zheltikov, *et al.*, J. Opt. Soc. Am. B **19**, 2183 (2002).

16. J. K. Ranka, R. S. Windeler, and A. J. Stentz, Opt. Lett. **25**, 25 (2000).
17. W. J. Wadsworth, A. Ortigosa-Blanch, J. C. Knight, *et al.*, J. Opt. Soc. Am. B **19**, 2148 (2002).
18. A. B. Fedotov, Ping Zhou, A. P. Tarasevitch, *et al.*, J. Raman Spectrosc. **33** (11/12), ?? (2002).
19. St. Coen, A. H. L. Chau, R. Leonhardt, *et al.*, Opt. Lett. **26**, 1356 (2001).
20. S. Coen, A. Hing Lun Chau, R. Leonhardt, *et al.*, J. Opt. Soc. Am. B **19**, 753 (2002).
21. A. B. Fedotov, A. N. Naumov, A. M. Zheltikov, *et al.*, J. Opt. Soc. Am. B **19**, 2156 (2002).
22. J. M. Dudley, Xun Gu, Lin Xu, *et al.*, Opt. Express **10**, 1215 (2002).
23. S. A. Diddams, D. J. Jones, Jun Ye, *et al.*, Phys. Rev. Lett. **84**, 5102 (2000).
24. D. J. Jones, S. A. Diddams, J. K. Ranka, *et al.*, Science **288**, 635 (2000).
25. R. Holzwarth, T. Udem, T. W. Hansch, *et al.*, Phys. Rev. Lett. **85**, 2264 (2000).
26. S. N. Bagayev, A. K. Dmitriyev, S. V. Chepurov, *et al.*, Laser Phys. **11**, 1270 (2001).
27. I. Hartl, X. D. Li, C. Chudoba, *et al.*, Opt. Lett. **26**, 608 (2001).
28. J. Herrmann, U. Griebner, N. Zhavoronkov, *et al.*, Phys. Rev. Lett. **88**, 173 901 (2002).
29. R. F. Cregan, B. J. Mangan, J. C. Knight, *et al.*, Science **285**, 1537 (1999).
30. S. O. Konorov, A. B. Fedotov, O. A. Kolevatova, *et al.*, Pis'ma Zh. Éksp. Teor. Fiz. **76**, 401 (2002) [JETP Lett. **76**, 341 (2002)].
31. A. N. Naumov and A. M. Zheltikov, Kvantovaya Élektron. (Moscow) **32**, 129 (2002).
32. F. Benabid, J. C. Knight, and P. St. J. Russell, Opt. Express **10**, 1195 (2002).
33. P. Yeh, A. Yariv, and E. Marom, J. Opt. Soc. Am. **68**, 1196 (1978).
34. Yong Xu, R. K. Lee, and A. Yariv, Opt. Lett. **25**, 1756 (2000).
35. G. Ouyang, Yong Xu, and A. Yariv, Opt. Express **9**, 733 (2001).
36. T. Kawanishi and M. Izutsu, Opt. Express **7**, 10 (2000).
37. S. G. Johnson, M. Ibanescu, M. Skorobogatiy, *et al.*, Opt. Express **9**, 748 (2001).
38. M. Ibanescu, Y. Fink, S. Fan, *et al.*, Science **289**, 415 (2000).
39. *Landolt–Börnshtein Physikalisch–Chemische Tabellen*, Ed. by W. A. Roth and K. Scheel (Springer, Berlin, 1931 and 1935), Vols. 2 and 3.
40. G. P. Agrawal, *Nonlinear Fiber Optics* (Academic, Boston, 1989; Mir, Moscow, 1996).
41. O. A. Kolevatova and A. M. Zheltikov, Laser Phys. (in press).
42. T. M. Monro, D. J. Richardson, N. G. R. Broderick, and P. J. Bennet, J. Lightwave Technol. **18**, 50 (2000).
43. A. M. Zheltikov and A. N. Naumov, Kvantovaya Élektron. (Moscow) **31**, 471 (2001).
44. G. Ouyang, Yong Xu, and A. Yariv, Opt. Express **10**, 899 (2002).
45. A. M. Zheltikov, Usp. Fiz. Nauk **172**, 743 (2002).
46. A. B. Fedotov, A. N. Naumov, I. Bugar, *et al.*, IEEE J. Sel. Top. Quantum Electron. **8**, 665 (2002).
47. A. B. Fedorov, I. Bugar, A. N. Naumov, *et al.*, Pis'ma Zh. Éksp. Teor. Fiz. **75**, 374 (2002) [JETP Lett. **75**, 304 (2002)].
48. A. Yariv and P. Yeh, *Optical Waves in Crystals: Propagation and Control of Laser Radiation* (Wiley, New York, 1984; Mir, Moscow, 1987).
49. E. A. J. Marcatili and R. A. Schmeltzer, Bell Syst. Tech. J. **43**, 1783 (1964).
50. A. B. Fedotov, F. Giammanco, A. N. Naumov, *et al.*, Appl. Phys. B **72**, 575 (2001).
51. O. A. Kolevatova, A. N. Naumov, and A. M. Zheltikov, Kvantovaya Élektron. (Moscow) **31**, 173 (2001).
52. A. R. McGurn, K. T. Christensen, F. M. Mueller, and A. A. Maradudin, Phys. Rev. B **47**, 13 120 (1993).
53. A. Kirchner, K. Busch, and C. M. Soukoulis, Phys. Rev. B **57**, 277 (1998).
54. A. A. Asatryan, P. A. Robinson, L. C. Botten, *et al.*, Phys. Rev. E **60**, 6118 (1999).
55. R. C. McPhedran, L. C. Botten, A. A. Asatryan, *et al.*, Phys. Rev. E **60**, 7614 (1999).
56. Chongjun Jin, Xiaodong Meng, Bingying Cheng, *et al.*, Phys. Rev. B **63**, 195 107 (2001).
57. Xiangdong Zhang and Zhao-Qing Zhang, Phys. Rev. B **65**, 245 115 (2002).

Translated by A. Zheltikov

SPELL: 1. fuzzily, 2. aperiodically, 3. tunability, *Stroitelei* or *Stroiteleĭ*—?